# Accepted Manuscript

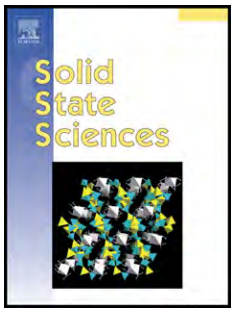


Superparamagnetic behavior and AC-losses in $NiFe_2O_4$ nanoparticles

O.V. Yelenich, S.O. Solopan, T.V. Kolodiazhnyi, V.V. Dzyublyuk, A.I. Tovstolytkin, A.G. Belous

PII: S1293-2558(13)00106-4

DOI: 10.1016/j.solidstatesciences.2013.03.013

Reference: SSSCIE 4717

To appear in: *Solid State Sciences*

Received Date: 12 November 2012

Revised Date: 28 December 2012

Accepted Date: 18 March 2013

Please cite this article as: O.V. Yelenich, S.O. Solopan, T.V. Kolodiazhnyi, V.V. Dzyublyuk, A.I. Tovstolytkin, A.G. Belous, Superparamagnetic behavior and AC-losses in $NiFe_2O_4$ nanoparticles, *Solid State Sciences* (2013), doi: 10.1016/j.solidstatesciences.2013.03.013.

$T_{synthesis}$ = 200°C SLP = 1.85 W/g

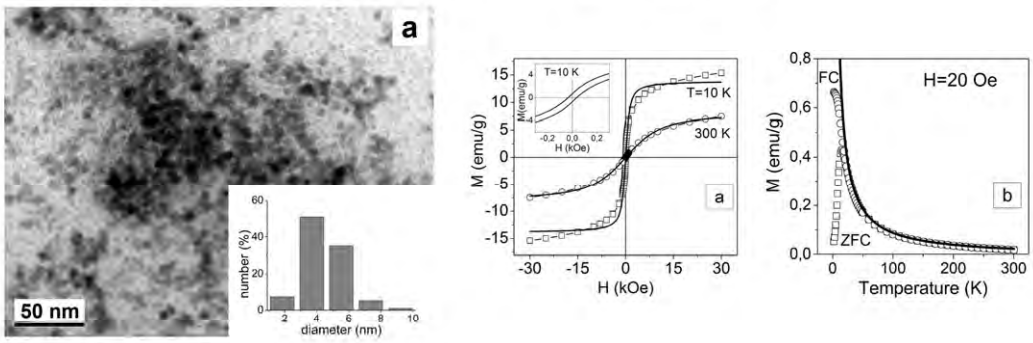


$T_{synthesis}$ = 500°C SLP = 206 W/g

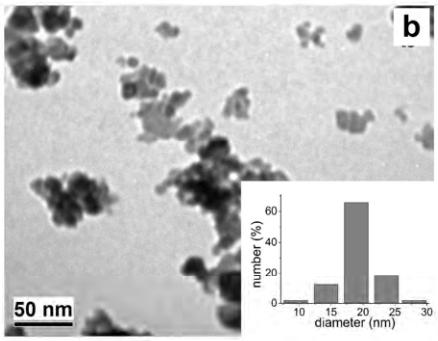

# SUPERPARAMAGNETIC BEHAVIOR AND AC-LOSSES IN $NiFe_2O_4$ NANOPARTICLES

O.V. Yelenich[1], S.O. Solopan[1,*], T.V. Kolodiazhnyi[2], V.V. Dzyublyuk[3], A.I. Tovstolytkin[3], A.G. Belous[1]

[1] Institute of General and Inorganic Chemistry, 32/34 Palladina Blvd., Kyiv 03142, Ukraine;

[2] National Institute for Materials Science, 1-1 Namiki, Tsukuba, Ibaraki 305-0044, Japan;

[3] Institute of Magnetism, 36-b Vernadsky Blvd., Kyiv 03142, Ukraine

**Abstract**

Crystallographic, microstructural and magnetic properties of $NiFe_2O_4$ nanoparticles synthesized by precipitation from nonaqueous solutions have been studied in the work. The transmission electron microscopy studies reveal particle sizes ~5 nm for the as-prepared particles which increase up to ~20 nm upon annealing at 500 $^oC$. Quasistatic magnetic measurements show superparamagnetic behavior with blocking temperature below room temperature for both the as-prepared and annealed particles. Characteristic magnetic parameters of the particles including average magnetic moment of an individual nanoparticle and effective anisotropy constant have been determined. The specific loss power which is released on the exposure of an ensemble of synthesized particles to an electromagnetic field is calculated and measured experimentally.

Keywords: nickel ferrite nanoparticles, superparamagnetic behavior, blocking temperature, AS-losses

[*] Corresponding author. Tel./fax: +380 44 4242211.
*E-mail*: solopan@ukr.net (S.O. Solopan).

## 1. Introduction

In recent years, nanocrystalline spinel-type oxides $MFe_2O_4$, where M is a divalent metal, have been receiving more attention due to their novel magnetic properties, which are significantly different from those of their bulk counterparts. These materials are technologically important and have been used in many applications including magnetic recording media and magnetic fluids for the storage and retrieval of information, magnetic resonance image enhancement, and others [1-4]. Of particular interest are also wide-range applications of ferrite nanoparticles in medicine, e.g. for drug delivery and hyperthermia in the treatment of cancer diseases [5].

Spinel-type oxides $MFe_2O_4$ are often denoted by the formula $AB_2O_4$ where A and B refer to tetrahedral and octahedral sites, respectively, in the fcc oxygen lattice [1,4,5]. These compounds often form a structure of inverse spinel, where $Fe^{3+}$ ions occupy A sites, whereas $M^{2+}$ and remaining $Fe^{3+}$ ions occupy B sites. It is known that at nanoscale level redistribution or inversion of cations between tetrahedral and octahedral sites may occur [1,4], which makes the investigations of nanocrystalline ferrites highly relevant.

Bulk nickel ferrite ($NiFe_2O_4$) is an inverse spinel. Like all soft magnetic ferrites, this compound is the subject of intense researches in recent years, especially in nanocrystalline state [4,6-8]. It has been shown in a series of works that $NiFe_2O_4$ nanoparticles can display superparamagnetic behavior in the vicinity of room temperature [6,7,8], which is especially important for the medical applications. The prospective of the use of nickel nanoferrites in medicine imposes additional requirements on the controllability of particles' size and parameters [1,9]. To date, however, the synthesis of monodisperse nanoparticles with controllable and reproducible parameters has remained a quite difficult task.

A large number of publications deals with the co-precipitation of slightly soluble compounds from aqueous solutions [10-13]. The formation of nanoparticles takes place with subsequent thermal decomposition of the resulting products to oxides. The complex and uncontrollable mechanism of such reactions involves crystal nucleation, growth, coarsening or agglomeration processes, which occur simultaneously. This often results in the agglomeration of nanoparticles.

In the references [14-18], $MFe_2O_4$ nanoparticles (M = Mn, Fe, Co, Ni, Zn) with spinel structure have been synthesized from metal chlorides in a diethylene glycol solution. The complex reaction of diethylene glycol with transition-metal cations makes it possible to separate in time the crystal nucleation and coarsening processes and, thus, to partially control the particles' size and aggregation.

At present, there is a strong demand for the magnetic nanoparticles with controllable size and narrow size distribution, because they may show considerable heating effects if subjected to magnetic AC-fields [1,5,9]. In particular, in magnetic particle hyperthermia proposed as a tumor therapy, magnetic nanoparticles are deposited in tumor tissue and are heated in an alternating magnetic field in order to destruct the tumor (for a review see Refs. [1,19]). However, despite the numerous empirical results on magnetic hyperthermia, there is no systematic understanding of the broad scattering of published data on the AC-losses in magnetic nanoparticles, as well as mechanisms of the losses (for a review see Refs. [19, 20]). There is also scarcity of data on the relation of the AC-losses to the magnetic parameters of a separate nanoparticle and its size.

The aim of this work was to study quasistatic magnetic properties and AC-losses in $NiFe_2O_4$ nanoparticles of different sizes synthesized by coprecipitation from a diethylene glycol solution using metal nitrates as starting reagents.

## 2. Experimental Section

For the synthesis of the $NiFe_2O_4$ nanoparticles, metal crystalline hydrates: $Fe(NO_3)_3 \cdot 6H_2O$, $Ni(NO_3)_2 \cdot 9H_2O$ (analytical grade), NaOH (purity 97%), diethylene glycol (DEG, purity 99%), oleic acid (pure OLA) were used as starting reagents. $NiFe_2O_4$ nanoparticles were synthesized in a three-neck flask in argon atmosphere. Two mmol of $Ni(NO_3)_2 \cdot 9H_2O$ and 4 mmol of $Fe(NO_3)_3 \cdot 6H_2O$ were dissolved in 40 mL of diethylene glycol, and the solution was stirred for 10-20 min. At the same time, a solution of 16 mmol of NaOH in DEG was prepared. The alkali solution was added to the mixture of the salts $Ni(NO_3)_2 \cdot 9H_2O$ and $Fe(NO_3)_3 \cdot 9H_2O$, and the resulting mixture was stirred for 2 h. The resulting solution was heat-treated at 200-220°C (60 min). In the next stage, oleic acid was added to the diethylene glycol solution, and the mixture was stirred for 10-20 min. The resulting colloidal solution was cooled and centrifuged. The isolated nanoparticles were washed with alcohol and dried in air at 30-50°C. Powders of ~0.4 g mass were obtained, which corresponds to a yield of 80-90%.

The nanopowders synthesized at 200°C were analyzed by means of IR spectroscopy (pellets with KBr). Samples were investigated by X-ray phase analysis (XPA) and full-profile X-ray phase analysis on a DRON-4 diffractometer (CuKα radiation). The size and morphology of powder particles have been determined by means of a JEM-1230 scanning electron microscope. To calculate size distribution were analyzed TEM images using the software of Image Tool 3.0. Magnetic measurements were performed in the 2-300 K temperature range using commercial Quantum Design Magnetic Property Measurements System equipped with superconducting quantum interference device (SQUID) . Magnetic moment was measured upon heating for both

zero-field-cooled (ZFC) and field-cooled (FC) conditions. Isothermal magnetic hysteresis loops were measured at 10 and 300 K in the magnetic field interval of -3 to +3 Tesla. For the calorimetric determination of specific loss power (SLP) the ferrofluids based on synthesized nanoparticles were prepared using 0.1 % aqueous agarose solutions [9] and placed into a coil that provides the alternating magnetic field (frequency 300 kHz, amplitudes up to 7.7 kA/m). The SLP was calculated using equation (1) [21],

$$SLP = \frac{C_{H_2O} \cdot V_S}{m_{NiFe_2O_4}} \cdot \frac{dT}{d\tau} \qquad (1)$$

where d$T$/d$\tau$ is the initial slope of the graph of the change in temperature versus time, $C_{H_2O}$ is the volumetric specific heat capacity of the sample solution, *Vs* is the sample volume and $m_{NiFe_2O_4}$ is the mass of magnetic material in the sample.

## 3. Results and discussion

### *3.1. Synthesis and microstructure*

As was shown earlier [22], nanoparticles are formed through processes of complex formation between metal cations and diethylene glycol molecules. The formation of complexes allows one to control crystal nucleation and coarsening with subsequent formation of nanoparticles. On the basis of the carried out investigations, appropriate mechanisms of the reactions proceeding in the system, which result in the formation of $NiFe_2O_4$ nanoparticles, have been drawn up. In the first stage, complex compounds are formed during the dissolution of $Ni(NO_3)_2$ and $Fe(NO_3)_3$ in diethylene glycol (scheme 1):

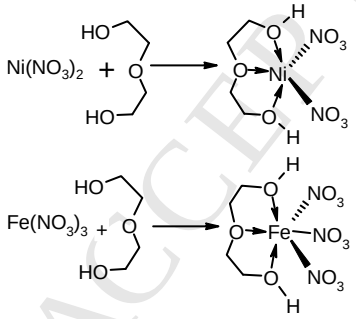


**(1)**

The subsequent addition of alkali results in the formation of dianionic metal complexes, which change into hydroxocomplexes in the presence of water (scheme 2).

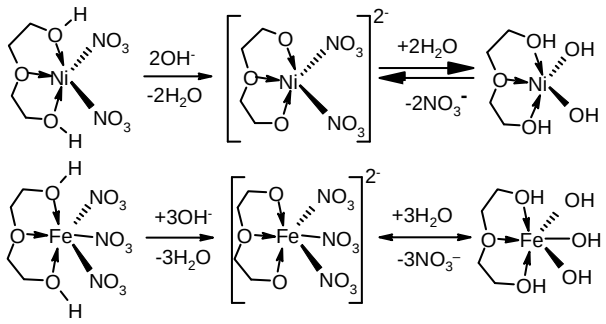

**(2)**

On heating the reaction mixture to 220°C, the complex compounds decompose, and $NiFe_2O_4$ nanoparticles with spinel structure are formed in accordance with the scheme 3

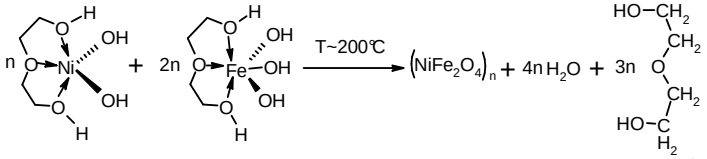

**(3)**

The formation of nanoparticles can be observed visually in the case of the reaction mixture becoming turbid with the formation of a dark-brown colloidal solution. Similar results were observed by the authors of [14] when using metal chlorides at starting reagents.

Figure 1 shows the results of IR spectroscopy of $NiFe_2O_4$ powder obtained after washing with absolute ethanol and dried at 50°C. Two broad absorption bands $\nu_1$ and $\nu_2$ at 560 $cm^{-1}$ and 380 $cm^{-1}$ are observed in the spectrum, which relate to the Me-O bond vibrations in tetra- and octahedral $NiFe_2O_4$ lattice sites [23].

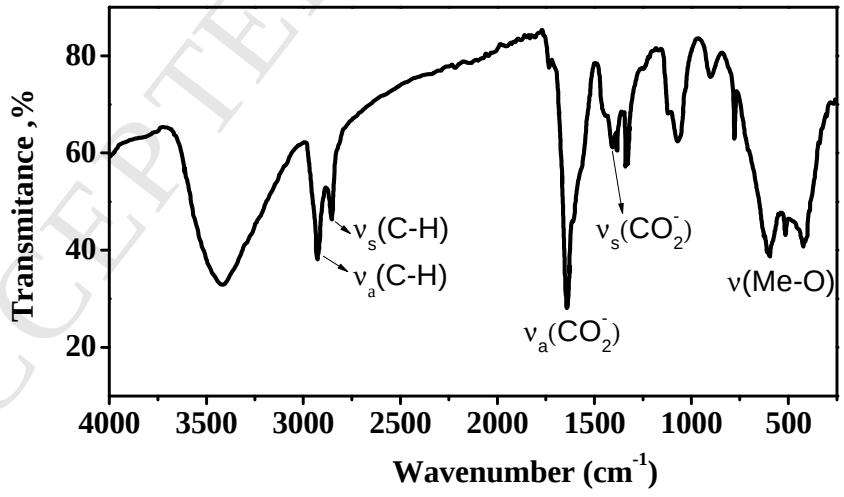


Fig. 1. IR spectra of $NiFe_2O_4$ nanopowders obtained from a diethylene glycol solution at 200°C.

Along with the pointed out peculiarities, characteristic lines at 1640 $cm^{-1}$ and 1400 $cm^{-1}$ are observed, which correspond to asymmetrical and symmetrical valence vibrations of carboxy anion, indicating the presence of remnants of oleic acid [24]. At the same time, absorption bands

at 2924 $cm^{-1}$ ($\nu_a$ C-H), 2853 $cm^{-1}$ ($\nu_s$ C-H), and 1405 $cm^{-1}$ ($\delta_a$ C-H), are observed, which may be assigned to carbon backbone vibrations of oleic acid or diethylene glycol [25].

The measured XRD data are shown in Fig. 2. The results indicate the formation of a single phase cubic spinel structure during synthesis at 200-220°C. Average particle diameter calculated from the half-width of the (311) peak by using Scherrer formula is equal to 6.6 nm. Cubic lattice parameters (a = 8.347 Å, $R_F$ = 3,47, $R_B$ = 2,92) have been calculated on the basis of the data of an XRD for nanoparticles synthesized at 200-220°C.

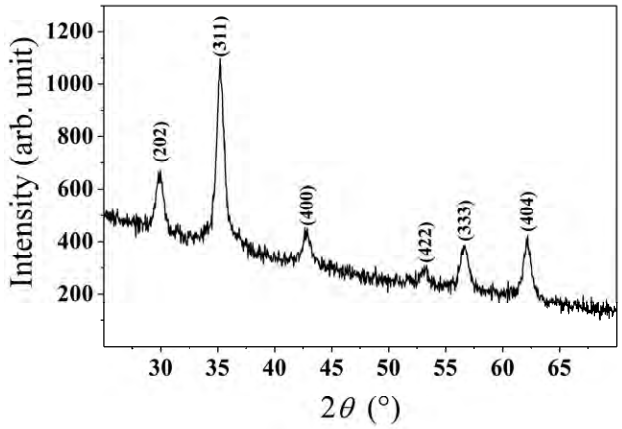


Fig. 2. X-ray diagram for $NiFe_2O_4$ nanoparticles obtained from a diethylene glycol solution at 200-220°C.

Figure 3 shows the results of the electron microscope investigations of the $NiFe_2O_4$ nanoparticles obtained from a diethylene glycol solution at 200-220°C (a) and nanoparticles annealed at 500°C under argon atmosphere (b). At 200-220°C we observe the formation of slightly agglomerated particles (ca 5 nm), which are characterized by a narrow size distribution with 95% of the particles having the size of 3-6 nm (inset in Fig 3a). Heat treatment of the $NiFe_2O_4$ nanoparticles at 500°C results in the increase in the particle size up to ~ 20 nm (Fig. 3b).

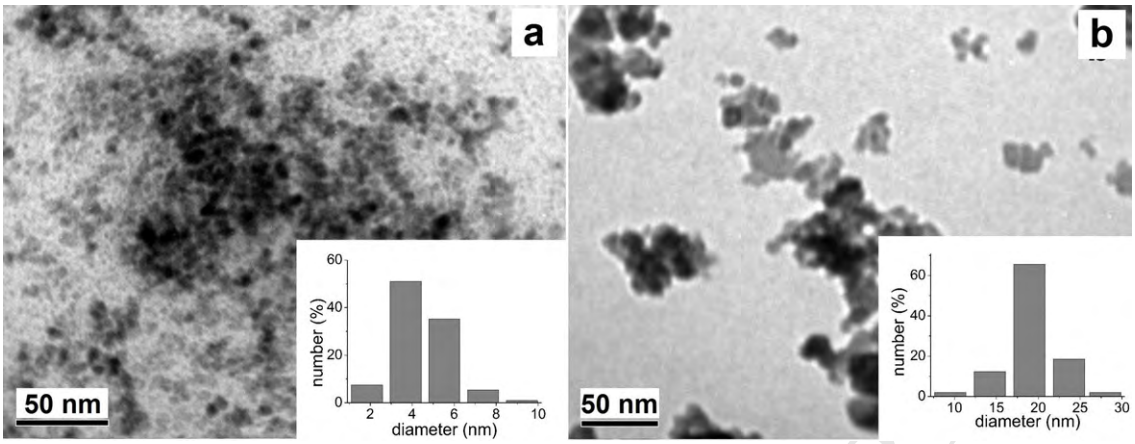


Fig. 3. TEM images of $NiFe_2O_4$ nanoparticles obtained from a diethylene glycol solution at 200 – 220°C (**a**) and annealed at 500°C (under argon) (**b**). Insets: size distribution diagram for $NiFe_2O_4$ nanoparticles.

### *3.2. Electophysical properties*

It should be noted that magnetic particles with the size less than a certain critical value [26] are single-domain, since the energy cost of domain wall formation outweighs any saving in demagnetizing energy [27]. The magnetization behavior of single-domain particles in thermodynamic equilibrium is identical to that of an atomic paramagnet and is called superparamagnetic [27]. If the magnetic moment of a single particle is $\mu$, the equilibrium magnetization $M$ for the ensemble of such particles placed in an external magnetic field $H$ at a given temperature $T$ is [28]:

$$M = n\mu L\left(\frac{\mu H}{kT}\right) \equiv n\mu\left[\coth\left(\frac{\mu H}{kT}\right) - \frac{kT}{\mu H}\right], \quad (2)$$

where $L$ is the Langevin function [28], $n$ is the concentration of particles, and $k$ is the Boltzmann constant.

Fig. 4 shows the *M(H)* dependences obtained for the ensemble of $NiFe_2O_4$ nanoparticles synthesized in this work. The measurements were carried out at $T$ = 300 K and 10 K. Solid lines in this figure present the results of the fitting of experimental data with formula (2). The fitting procedure was carried out with the use of a fitting tool of OriginPro 8.5 SR1. At 300 K, the fitted curve well corresponds to the experimental dependence, which makes it possible to calculate the magnetic moment of a single superparamagnetic particle $\mu \approx 9.6 \cdot 10^{-18}$ erg/G ($\mu = 1.01 \cdot 10^3$ $\mu_B$, where $\mu_B$ is the Bohr magneton) and particle concentration: $n \approx 1.03 \times 10^{19}$ $cm^{-3}$. Thus, one

magnetic particle occupies a volume of $9.7\times10^{-20}$ cm$^3$, which corresponds to the particle diameter $d$ = 5.7 nm.

The average particle diameter calculated from the data of magnetic measurements well agrees with the results of electron microscopy investigations (see Fig. 3a) and powder X-ray analysis (see above). Such correspondence additionally confirms that the distribution in particle size is quite narrow. On the other hand, this fact also provides evidence that the whole volume of the particle is magnetically ordered.

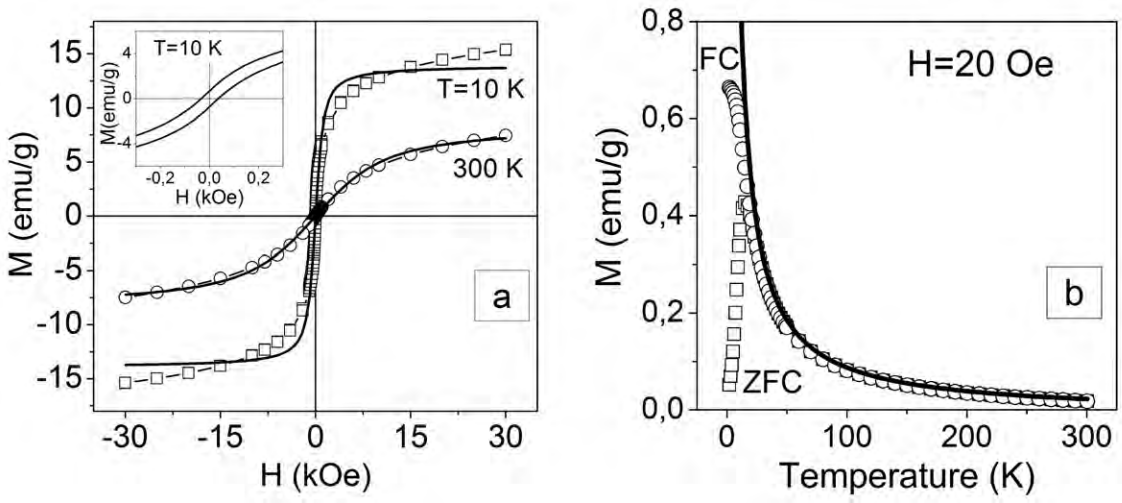


Fig. 4. The $M$ vs $H$ dependences measured at 300 K and 10 K for the $NiFe_2O_4$ powder (**a**) and temperature dependences of $M_{ZFC}$ and $M_{FC}$ obtained in 20 Oe probing field (**b**). Open circles and squares show experimental data, solid lines – the curves fitted with formula (2). Inset shows the *M(H)* hysteresis at 10 K within a low field region.

The application of formula (2) to the *M(H)* dependence obtained at 10 K does not demonstrate satisfactory agreement with the experiment. The fitted curve (solid line in Fig. 4(a)), which corresponds to $\mu$ = 2.87 $\cdot10^{-18}$ erg/G, $n$ = $2.5\times10^{19}$ cm$^{-3}$, cannot be considered as satisfactory for the description of experimental results. The reason for such discrepancy may be related to the enhanced role of the particles' anisotropy energy at low temperatures [27]. The hysteresis character of the *M(H)* curve (see inset in Fig. 3a) agrees with this statement. At 300 K much better fit is obtained partially due to the fact that the anisotropy energy is much smaller than $kT$.

Figure 4b shows temperature dependences of magnetization, obtained in two different measurement modes. The $M_{ZFC}(T)$ curve was obtained by heating the powder in 20 Oe probing field after its preliminary cooling in zero magnetic field ($H_{ext}$ = 0) from room temperature to 2 K. To obtain the $M_{FC}(T)$ dependence, the powder was cooled in $H_{ext}$ = 20 Oe and then the measurements were carried out during heating the powder in the same field.

As seen from Fig. 4b, the $M_{ZFC}(T)$ dependence displays a maximum at $T_B$ = 15 K, which is called a blocking temperature. The appearance of the maximum on the $M_{ZFC}(T)$ curve indicates that the anisotropy energy of the nanoparticles, $KV$ ($K$ is the effective anisotropy constant and $V$ is the particle volume), becomes comparable to the thermal energy $kT$ [27]. As a result, at $T \leq T_B$, the orientation of the magnetic moments of the particles is governed by the anisotropy energy (blocked state), rather than the thermal energy or the energy of small external magnetic field [27-29].

Solid line in Fig. 4b shows $M(T)$ dependence calculated according to formula (2) ($H$ = 20 Oe and $T$ = var). For these calculations, the parameters ($\mu$ = 9.6 $\cdot 10^{-18}$ erg/G, $n$ = $1.03\times10^{19}$ $cm^{-3}$) were used, which were derived from the fitted $M(H)$ dependence at 300 K. One can see that the calculated and experimental curves practically coincide in the vicinity of room temperature. However, the curves diverge at low temperatures which is also indicative of the enhanced role of the anisotropy energy as a result of a decrease of the thermal energy $kT$ [30].

Having found blocking temperature $T_B$ from the $M_{ZFC}(T)$ curve, one can estimate the effective anisotropy constant with the use of formula [31]:

$$K = \frac{25kT_B}{V} . \qquad (3)$$

For the $NiFe_2O_4$ nanoparticles under consideration, the value of $K$ calculated in such a way is $23.34\times10^4$ erg/$cm^3$ ($2.334\times10^4$ J/$m^3$).

The AC-losses for the $NiFe_2O_4$ nanoparticles placed in an external electromagnetic field were calculated with the use of the linear response theory using the Neel - Brown relaxation time [21, 32]. This model is based on the assumption that the magnetic system responds linearly with the magnetic field and is suitable for calculation of AC-losses in superparamagnetic nanoparticles at low magnetic field [20]. According to this model, the specific loss power (SLP) can be expressed as

$$P = \mu_0 \chi H_0^2 \frac{2\pi^2 f^2 \tau}{1+(2\pi f\tau)^2}, \qquad (4)$$

where $\mu_0$ is the permeability of free space ($\mu_0 = 4\pi \times 10^{-7}$ N/m), $\chi$ – the magnetic susceptibility of the powder, $H_0$ – the intensity of magnetic field, and $f$ – the frequency of electromagnetic field. For the ensemble of superparamagnetic particles possessing magnetic moment $\mu$, magnetic susceptibility can be calculated using formula [27,30]:

$$\chi = n\frac{\mu_0\mu^2}{3kT} . \qquad (5)$$

The relaxation time can be written in the form [32]:

$$\tau = \frac{\sqrt{\pi}}{2}\tau_0 \frac{\exp(\Gamma)}{\sqrt{\Gamma}}, \qquad (6)$$

where $\Gamma = \frac{KV}{kT}$ and $\tau_0 = 10^{-9}$ s [32].

The SLP was calculated for the $NiFe_2O_4$ nanopowder placed in electromagnetic field with $f$ = 300 kHz and $H_0$ = 7.7 kA/m (98 Oe). Magnetic susceptibility, $\chi$, calculated for the $NiFe_2O_4$ powder with employing formulae (2) and (5), is $3.2\times10^{-7}$ $g^{-1}$. The value of $\tau$ is $2.77\times10^{-8}$ s (see expression (6)). As a result, $P$ = 1.36 W/g.

These data well agree with the experimental results obtained for the $NiFe_2O_4$ nanopowder synthesized in this work: for $f$ = 300 kHz and $H_0$ = 7.7 kA/m (98 Oe), the experimental value of $P$ is 1.85 W/g.

The method of the synthesis of nanoparticles, employed in this work allows one to control the growth processes and, thus, to purposefully change the parameters of the obtained materials. The analysis of formulae (4)-(6) makes it possible to find out which experimental direction is the most efficient for enhancement of $P$.

It is seen from expressions (4)-(6) that the SLP is very sensitive to the particle volume. So, the increase in $V$ gives rise to the increase in both magnetic susceptibility $\chi$ and relaxation time, $\tau$, which is expected to lead to a substantial enhancement of $P$.

Investigations carried out in this work have shown that the heat treatment of the $NiFe_2O_4$ nanoparticles at 500 °C results in the increase in the particle size up to ~ 20 nm (Fig. 3b). It should be noted that after such treatment, a partial agglomeration of particles occurs and the magnetization no longer obeys the Langevin function. This makes invalid the use of the above approach to calculate the SLP. At the same time, the experimentally measured SLP value for the nanoparticles subjected to such a treatment is 206 W/g, which is far greater than for the as-prepared nickel nanoferrite.

As a result, the synthesis of $NiFe_2O_4$ from non-aqueous solutions makes it possible to obtain weakly agglomerated nanoparticles, the size and properties of which can be varied over a wide range. This is both of fundamental and applied interest for the use of the synthesized particles in medicine for a wide range of purposes.

## 4. Conclusion

In this work, weakly agglomerated nanoparticles of $NiFe_2O_4$ compound with different particle sizes have been synthesized by the method of co-precipitation from nonaqueous solutions with the use of metal nitrites as starting reagents. The particles display a narrow size

distribution and are superparamagnetic at 300 K. Characteristic magnetic parameters of the particles including average magnetic moment of an individual nanoparticle and effective anisotropy constant have been determined in the work. The specific loss power which is released on the irradiation of an ensemble of particles with an electromagnetic field has been calculated and measured experimentally. It has been shown that the proposed synthesis procedure allows a wide-range control of the size and properties of $NiFe_2O_4$ nanoparticles.

## References


[1] S.P. Gubin, Magnetic Nanoparticles, Wiley-VCH, Weinheim, 2009.

[2] T. Misu, N. Sakamoto, K. Shinozaki, N. Adachi, H. Suzuki, N. Wakiya, Magnetic and optical properties of $MgAl_2O_4$-$(Ni_{0.5}Zn_{0.5})Fe_2O_4$ thin films prepared by pulsed laser deposition, Sci. Technol. Adv. Mater. 12 (2011) 034408.

[3] B.S. Inbaraj, T.-Y. Tsai, B.-H. Chen, Synthesis, characterization and antibacterial activity of superparamagnetic nanoparticles modified with glycol chitosan, Sci. Technol. Adv. Mater. 13 (2012) 015002.

[4] R.D.K. Misra, S. Gubbala, A. Kale, W.F. Egelhoff Jr., A comparison of the magnetic characteristics of nanocrystalline nickel, zinc, and manganese ferrites synthesized by reverse micelle technique, Materials Science and Engineering B 111 (2004) 164–174.

[5] B.E. Kashevsky, V.E. Agabekov, S.B. Kashevsky, K.A. Kekalo, E.Y. Manina, I.V. Prokhorov, V.S. Ulashchik, Study of cobalt ferrite nanosuspensions for low-frequency ferromagnetic hyperthermia, Particuology 6 (2008) 322–333.

[6] T.F. Marinca, I. Chicinas, O. Isnard, V. Pop, F. Popa, Synthesis, structural and magnetic characterization of nanocrystalline nickel ferrite - $NiFe_2O_4$ obtained by reactive milling, J. Alloys and Compounds 509 (2011) 7931-7936.

[7] R. Malik, S. Annapoorni, S. Lamba, V. Raghavendra Reddy, A. Gupta, P. Sharma, A. Inoue, Mössbauer and magnetic studies in nickel ferrite nanoparticles: Effect of size distribution, J. Magn. Magn. Mater. 322 (2010) 3742-3747

[8] V. Sepelak, M. Menzel, I. Bergmann, M. Wiebcke, F. Krumeich, K.D. Becker, Structural and magnetic properties of nanosize mechanosynthesized nickel ferrite, J. Magn. Magn. Mater. 272–276 (2004) 1616–1618.

[9] S. Solopan, A. Belous, A. Yelenich, L. Bubnovskaya, A. Kovelskaya, A. Podoltsev, I. Kondratenko, S. Osinsky, Nanohyperthermia of malignant tumors. I. Lanthanum-strontium manganite magnetic fluid as potential inducer of tumor hyperthermia, Experimental Oncology 33 (2011) 130–135.

[10] M.M. El-Okr, M.A. Salema, M.S. Salim, R.M. El-Okr, M. Ashous, H.M. Talaat, Synthesis of cobalt ferrite nano-particles and their magnetic characterization, J. Magn. Magn. Mater. 323 (2011) 920.

[11] K. Maaz, Arif Mumtaz, S.K. Hasanain, Abdullah Ceylan, Synthesis and magnetic properties of cobalt ferrite ($CoFe_2O_4$) nanoparticles prepared by wet chemical route, J. Magn. Magn. Mater. 308 (2007) 289.

[12] H. Iida, K. Takayanagi, T. Nakanishi, T. Osaka, Synthesis of $Fe_3O_4$ nanoparticles with various sizes and magnetic properties by controlled hydrolysis, Journal of Colloid and Interface Science 314 (2007) 274–280.

[13] K. Velmurugan, V.S.K. Venkatachalapathy, S. Sendhilnathan, Synthesis of nickel zinc iron nanoparticles by coprecipitation technique, Materials Research 13 (2010) 299–303.

[14] B.L. Cushing, V.L. Kolesnichenko, and C.J. O'Connor, Recent advances in the liquid-phase syntheses of inorganic nanoparticles, Chemical Reviews 104 (2004) 3893–3946.

[15] C. Feldmann, Polyol-mediated synthesis of nanoscale functional materials, Adv. Funct. Mater. 13 (2003) 101–107.

[16] Existing Chemical Hazard Assessment Report, June 2009.

[17] D. Caruntu, Y. Remond, N.H. Chou, M.-J. Jun, G. Caruntu, J. He, G. Goloverda, C. O'Connor, and V. Kolesnichenko, Reactivity of 3d transition metal cations in diethylene glycol solutions. Synthesis of transition metal ferrites with the structure of discrete nanoparticles complexed with long-chain carboxylate anions, Inorg. Chem. 41 (2002) 6137–6146.

[18] G. Goloverda, B. Jackson, C. Kidd, V. Kolesnichenko, Synthesis of ultrasmall magnetic iron oxide nanoparticles and study of their colloid and surface chemistry, J. Magn. Magn. Mater. 321 (2009) 1372–1376.

[19] R. Hergt, S. Dutz, R. Müller and M. Zeisberger, Magnetic particle hyperthermia: nanoparticle magnetism and materials development for cancer therapy, J. Phys.: Condens. Matter. 18 (2006) S2919–S2934.

[20] J. Carrey, B. Mehdaoui, and M. Respaud, Simple models for dynamic hysteresis loop calculations of magnetic single domain nanoparticles: Application to magnetic hyperthermia optimization, J. Appl. Phys. 109 (2011) 083921 (18 pages).

[21] J.-H. Lee, Jung-tak Jang, Jin-sil Choi, Seung Ho Moon, Seung-hyun Noh, Ji-wook Kim, Jin-Gyu Kim, Il-Sun Kim, Kook In Park & Jinwoo Cheon, Exchange-coupled magnetic nanoparticles for efficient heat induction, Nature Nanotechnology 6 (2011) 418–422.

[22] A.G. Belous, O.V. Yelenich, S.O. Solopan, V.V. Trachevskii, Synthesis and properties of $AFe_2O_4$ nanoparticles (A = Mn, Fe, Co, Ni, Zn) obtained by precipitation from a diethylene glycol solution, Journal of Inoraganic Chemistry 2012 (In press).

[23] P. Sivakumar R. Ramesh, A. Ramanand, S. Ponnusamy, C. Muthamizhchelvan, Preparation of sheet like polycrystalline NiFe2O4 nanostructure with PVA matrices and their properties, Materials Letters 65 (2011) 1438–1440.

[24] L. Zhang, R. He, H.-C. Gu, Oleic acid coating on the monodisperse magnetite nanoparticles, Applied Surface Science 253 (2006) 2611–2617.

[25] S.Y. Lee, M.T. Harris, Surface modification of magnetic nanoparticles capped by oleic acids: Characterization and colloidal stability in polar solvents, J. Colloid Interface Sci. 293 (2006) 401-408.

[26] R. K. Das, S. Rawa, D. Norton,and A. F. Hebard, A collective dynamics description of dipolar interactions and the coercive field of magnetic nanoparticles, J. Appl. Phys. 108 (2010) 123920.

[27] S. Bedanta and W. Kleemann, Supermagnetism, J. Phys. D: Appl. Phys. 42 (2009) 013001.

[28] W.T. Coffey, Y.P. Kalmykov and J.T. Waldron, The Langevin Equation, World Scientific, Singapore, 1996.

[29] I. García, J. Echeberria, G.N. Kakazei, V.O. Golub, O.Y. Saliuk, M. Ilyn, K.Y. Guslienko, J.M. Gonzílez, Evolution of the Magnetic Properties of $Co_{10}Cu_{90}$ Nanoparticles Prepared by Wet Chemistry with Thermal Annealing, Journal of Nanoscience and Nanotechnology 12 (2012) 7529–7534.

[30] S. Chikazumi, C.D.Jr. Graham, Physics of Ferromagnetism, Oxford University Press, New York, 2009.

[31] H. Nathani, S. Gubbala, R.D.K. Misra, Magnetic behavior of nanocrystalline nickel ferrite Part I. The effect of surface roughness, Mater. Sci. Eng. B 121 (2005) 126–136.

[32] R. E. Rosensweig, Heating magnetic fluid with alternating magnetic field, J. Magn. Magn. Mater. 252 (2002) 370–374.

**Figure captions**

Fig. 1. IR spectra of $NiFe_2O_4$ nanopowders obtained from a diethylene glycol solution at 200°C.

Fig. 2. X-ray diagram for $NiFe_2O_4$ nanoparticles obtained from a diethylene glycol solution at 200-220°C.

Fig. 3. TEM images of $NiFe_2O_4$ nanoparticles obtained from a diethylene glycol solution at 200 – 220°C (a) and annealed at 500°C (under argon) (b). Insets: size distribution diagram for $NiFe_2O_4$ nanoparticles.

Fig. 4. The *M* vs *H* dependences measured at 300 K and 10 K for the $NiFe_2O_4$ powder (a) and temperature dependences of $M_{ZFC}$ and $M_{FC}$ obtained in 20 Oe probing field (b). Open circles and squares show experimental data, solid lines – the curves fitted with formula (1). Inset shows the *M(H)* hysteresis at 10 K within a low field region.